Cell Proliferation

Cell Prolif., 2014, **47**, 553–563 doi: 10.1111/cpr.12141

Establishment of a three-dimensional culture system of gastric stem cells supporting mucous cell differentiation using microfibrous polycaprolactone scaffolds

S. Pulikkot*,†, Y. E. Greish†, A-H. I. Mourad‡ and S. M. Karam*

**Department of Anatomy, College of Medicine and Health Sciences, United Arab Emirates University, Al Ain, United Arab Emirates, †Department of Chemistry, College of Science, United Arab Emirates University, Al Ain, United Arab Emirates and ‡Department of Mechanical Engineering, College of Engineering, United Arab Emirates University, Al Ain, United Arab Emirates*

Received 19 April 2014; revision accepted 2 August 2014

Abstract

Objectives: To generate various polycaprolactone (PCL) scaffolds and test their suitability for growth and differentiation of immortalized mouse gastric stem (mGS) cells.

Materials and methods: Non-porous, microporous and three-dimensional electrospun microfibrous PCL scaffolds were prepared and characterized for culture of mGS cells. First, growth of mGS cells was compared on these different scaffolds after 3 days culture, using viability assay and microscopy. Secondly, growth pattern of the cells on microfibrous scaffolds was studied after 3, 6, 9 and 12 days culture using DNA PicoGreen assay and scanning electron microscopy. Thirdly, differentiation of the cells grown on microfibrous scaffolds for 3 and 9 days was analysed using lectin/immunohistochemistry.

Results: The mGS cells grew preferentially on microfibrous scaffolds. From 3 to 6 days, there was increase in cell number, followed by reduction by days 9 and 12. To test whether the reduction in cell number was associated with cell differentiation, cryosections of cell-containing scaffolds cultured for 3 and 9 days were probed with gastric epithelial cell differentiation markers. On day 3, none of the markers examined bound to the cells. However by day 9, approximately, 50% of them bound to *N*-acetyl-D-glucosamine-specific lectin and anti-trefoil factor 2 antibodies, indicating their differentiation into glandular mucus-secreting cells.

Conclusions: Microfibrous PCL scaffolds supported growth and differentiation of mGS cells into mucus-secreting cells. These data will help lay groundwork for future experiments to explore use of gastric stem cells and PCL scaffolds in stomach tissue engineering.

Correspondence: Y. E. Greish, Department of Chemistry, College of Science, United Arab Emirates University, Al Ain PO Box 15551, United Arab Emirates. Tel.: +971 3 713 6141; Fax: +971 3 713 4928; E-mail: y.afifi@uaeu.ac.ae and S. M. Karam, Department of Anatomy, College of Medicine and Health Science, United Arab Emirates University, Al-Ain PO Box 17666, United Arab Emirates. Tel.: +971 3 713 7493; Fax: +971 3 767 2033; E-mail: skaram@uaeu.ac.ae

Introduction

Glandular epithelia of mouse and human stomachs undergo continuous renewal. Multipotential stem/progenitor cells residing in each gastric gland actively divide to maintain themselves and to produce four main cell lineages secreting mucus, acid, pepsinogen and various hormones and peptides (1,2). Blocking production of acid-secreting parietal cells in a genetically engineered mouse model leads to amplification of gastric stem cells and their immediate descendants (3). This animal model has made it possible to establish a cell line representative of mouse gastric stem (mGS) cells (4). Characterization of these immortalized cells has demonstrated their undifferentiated morphology and their expression of some stem cell-specific genes: *Notch3*, *DCAMKl1* and *Oct4* (5,6).

In humans, alteration of the dynamic program of gastric epithelial stem cells precedes development of gastric cancer (7). This fatal tumour represents a common cancer in many countries (8). Although gastrectomy has contributed to improved survival for gastric cancer patients when diagnosed early, frequently used reconstructions remain inadequate, quality of life is poor

and morbidity is a major problem (9). Recent developments in tissue engineering could provide possibilities for improving quality of life following gastrectomy (10).

The principles of tissue engineering have been considered for replacement of resected cancer tissues by using stem cells that are capable of growth and differentiation on specially designed synthetic material (scaffold), to restore structure and function of the organ. An ideal scaffold for tissue engineering is a three-dimensional (3D) construct characterized by its biocompatibility, biodegradability and mechanical stability. Growth and differentiation of cells seeded on such scaffolds will indicate their suitability (or not) to be implanted *in vivo* for tissue replacement (11,12). Polycaprolactone (PCL) is one of these biodegradable polymers that has been extensively studied for various biomedical applications (13–15). PCL polymer has been found to be very promising for growth and differentiation of different types of stem cell in both soft and hard tissues (16–18).

For gastric tissue engineering, autologous gastric organoids have been proposed (19–22). In these studies, investigators used artificial scaffolds to support growth and differentiation of heterogeneous populations of isolated gastric mucosal fragments, made of a mesenchymal core surrounded by epithelia. However, none of them used a homogeneous population of gastric stem cells.

The aims of this investigation were as follows: (i) to generate and characterize various forms of PCL scaffold, (ii) to test growth and viability of mGS cells on the scaffolds and (iii) to assay proliferation and differentiation of mGS cells on the most suitable form of PCL scaffold for possible use in gastric epithelial tissue engineering.

Materials and methods

Fabrication of PCL scaffolds

Synthetic PCL, molecular weight (M_n) 70,000–90,000 by GPC (Sigma-Aldrich, St. Louis, MO, USA) was used as starting material for scaffold preparation. Initially, a homogeneous solution containing 25% PCL (w/v) in chloroform was used as a stock solution for preparation of three different forms of scaffold: (i) Non-porous PCL scaffolds prepared by casting 10 ml stock solution into a flat Petri dish which was then left in the air to dry, (ii) Microporous PCL scaffolds prepared by casting 10 ml PCL solution containing 50 wt% NaCl (average size of ≤50 μm), as porogen, in a flat Petri dish, then air dried. Each PCL sheet being then soaked in de-ionized water and stirred, to leach out NaCl granules leaving behind a microporous scaffold and (iii) Microfibrous PCL scaffolds prepared using an electrospinning technique (23,24). Briefly, 10 ml 25% PCL solution was spun at 12 kV, spinning distance 14 cm, and feed rate 0.16 ml/min. Electrospun PCL scaffolds were kept in air to ensure complete dryness. All scaffolds were sterilized by immersion in 70% ethanol for 60 min followed by 60-min exposure to UV light and three washes in sterile phosphate-buffered saline (PBS).

Characterization of PCL scaffolds

Morphologies of the prepared scaffolds were evaluated using a scanning electron microscope (SEM; XL-30 Phillips, Amsterdam, Netherlands) at accelerating voltage of 15 kV. Morphological features of the non-porous, microporous and microfibrous scaffolds were studied. Mechanical properties of the synthetic scaffolds were studied and compared to that of mouse stomach tissue. Tensile strengths and fracture strains were measured for the three types of scaffold using a 5 kN material testing system. All tests were conducted at room temperature and under displacement controlled conditions with 1 mm/min overhead speed. Calliper measurements were used to determine scaffold thickness. Scaffolds were cut into rectangular strips 5 × 2 cm. Tensile strength measurements were carried out in triplicate according to published procedures (25,26). For comparison, 6-month-old C57BL/6 mouse stomach tissues ($n = 3$) were collected, washed in cold PBS and immediately tested for their tensile strength.

Experiment 1: culture of mGS cells on different PCL scaffolds for 3 days. A frozen aliquot of mGS cells was thawed and seeded in a tissue culture flask containing 10% serum in RPMI culture medium. Establishment and characterization of the mGS cell line has been described previously (4). Cells were allowed to proliferate until semi-confluent in a 37 °C incubator adjusted to 5% CO_2, 95% O_2, culture medium being changed every other day. Cells were passaged twice to stabilize their morphology and growth rate. The mGS cells were then seeded (1.6×10^5 cells) on each sterilized non-porous, microporous and microfibrous PCL scaffold (5 mm in diameter) placed in a 96-well plate. After 3 days submerged culture, cells were processed in triplicate for different procedures: (i) Viability assay: cells incubated for 30 min in 2 μM calcein at 37 °C. Absorbance of calcein was detected at 485–535 nm using a VICTOR™ X3 PerkinElmer 2030 multilabel plate reader, (ii) Toluidine blue staining for light microscopy: cells were fixed in 4% paraformaldehyde for 15 min, washed in PBS, then incubated in 1% toluidine blue solution for 30 sec. Cells on the different scaffolds were then washed in double-

distilled water and examined using an inverted microscope (Olympus, Tokyo, Japan) and (iii) SEM: To examine surface morphology of cells grown on different PCL scaffolds, they were fixed in 4% paraformaldehyde for 15 min, washed in PBS and post-fixed in 1% osmium tetroxide for 10 min. Following dehydration in ascending grades of ethanol, cells were coated with gold–palladium and finally examined using a Phillips SEM.

Experiment 2: culture of mGS cells on microfibrous PCL scaffolds for 3–12 days. The mGS cells were suspended in serum-containing RPMI and seeded (2.5×10^5 cells) on to pre-sterilized microfibrous PCL scaffolds (15 mm diameter, 0.9 mm thickness) placed in a 12- or 24-well tissue culture plate and allowed to grow in a 37 °C incubator containing 5% CO_2 and 95% O_2, culture medium being changed every other day. After 3, 6, 9 and 12 days, cultured cells were analysed using a PicoGreen assay for quantification of DNA. Cells were washed in PBS and stored at −80 °C in 1 ml Milli-Q water. DNA was extracted from the samples by repeated freeze-thaw cycles followed by ultrasonication using a Sonic Ruptor 250 Ultrasonic Homogenizer (Omni International, Kennesaw, GA, USA). For quantification of DNA, Quant-iT PicoGreen dsDNA kit (Invitrogen, Eugene, OR, USA) was used according to the manufacturer's instructions. Briefly, a five-point standard curve of 1000, 100, 10, 1 and 0 ng/ml Lambda DNA was prepared. Following 5 min incubation of sonicated samples with the PicoGreen dye at room temperature, intensity of fluorescence was measured at 520 nm on the Perkin-Elmer reader. Scaffolds without cells were used as blank samples.

Experiment 3: culture of mGS cells on microfibrous PCL scaffolds for 3 and 9 days. The mGS cells were suspended in serum-containing RPMI and seeded on microfibrous PCL scaffolds placed in a 12- or 24-well tissue culture plate similar to that described in experiment 2. Cells were analysed after 3 and 9 days culture as follows: (i) SEM: To examine changes that had occurred in their morphology when grown on microfibrous PCL scaffolds for 9 days, cells were fixed in paraformaldehyde and processed for SEM as mentioned in experiment 1 and (ii) Cryostat sectioning and multi-label immuno-/lectin fluorescence cytochemistry: Cells grown on scaffolds for 3 and 9 days were fixed in 4% paraformaldehyde for 15 min. Following three PBS washes, cells attached to scaffolds were incubated in 20% buffered sucrose overnight at 4 °C. Cell-containing scaffolds were then mounted on an aluminium stalk using Shandon cryomatrix (Thermo Fisher Scientific, Waltham, MA, USA) and orientated perpendicular to the plane of sectioning. Samples were then dipped into liquid nitrogen for a few seconds. Using a cryostat, 10–30 μm-thick sections were obtained and mounted on gelatin-coated slides. Some cryosections were stained with haematoxylin and eosin and adjacent sections were probed with various biomarkers. As control, mGS cells grown on coverslips or chamber slides were probed with lectins and antibodies.

To obtain evidence of gastric stem cell differentiation, lectin binding and immunocytochemistry were performed on cryosections of cells grown on scaffolds for 3 and 9 days. Following incubation with blocking solution (1% bovine serum albumin in PBS) for 60 min, cells were incubated overnight with the following gastric cell lineage-specific antibodies: anti-H,K-ATPase antibody (specific for parietal cells; Medical & Biological Laboratories Co., Nagoya, Japan), anti-trefoil factor (TFF) 1 antibody (for mucous pit cells; gift from Catherine Tomasetto, IGBMC, Strasbourg, France), anti-TFF2 antibody (for glandular mucous cells; gift from Catherine Tomasetto, IGBMC), and anti-chromogranin antibody (for enteroendocrine cells; DAKO, Glostrup, Denmark). Probed sections were washed in PBS and appropriate biotinylated anti-mouse or anti-rabbit immunoglobulin G was added as secondary antibody. Finally, Alexa Fluor (555 or 488)-conjugated avidin was added to visualize antigen–antibody binding sites, using fluorescence Olympus or Nikon Eclipse 80i confocal microscopes (Tokyo, Japan). Cryosections of the cells were also incubated for 60 min with fluorophore-conjugated *Ulex europaeus* agglutinin (UEA) I lectin (specific for mucous pit cells), *Dolichos biflorus* agglutinin (DBA) lectin (for parietal cells) or *Griffonia simplicifolia* (GS)II lectin (for mucous neck cells) (27,28). All lectins were purchased from Sigma (St. Louis, MO, USA).

Statistical analysis

To test significance of data obtained from experiments 1 and 2, one-way ANOVA with Dunnet or Newman–Keuls Multiple Comparison Test models were employed. Graphical representation of the data (mean ± SD) was performed using GraphPad Prism software (La Jolla, CA, USA).

Results

Characterization of PCL scaffolds

Scanning electron microscope examination of the non-porous scaffolds revealed the surface morphology to have patterned irregularities probably due to evaporation

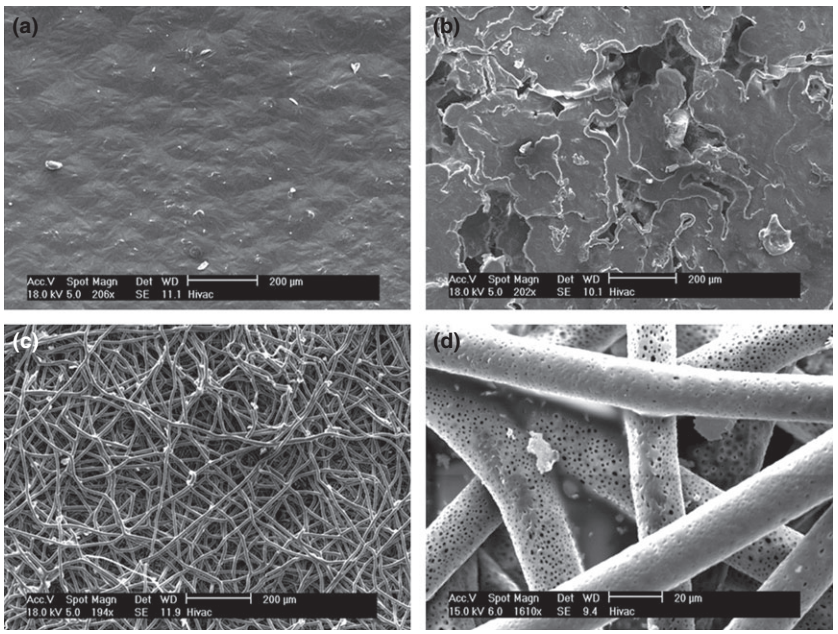

Figure 1. Scanning electron micrographs of non-porous (a), microporous (b) and microfibrous (c, d) scaffolds showing their surface topography. Note moderate roughness of the non-porous scaffold (a). The microporous scaffold appeared to have numerous pores, variable in size and frequently appearing to be interconnected (b). The microfibrous scaffold appeared as a complex meshwork of microfibres which were variable in thickness (c) and reveals some surface roughness (d). Bar = 200 µm (a–c), 20 µm (d).

of the solvent during air-drying (Fig. 1a). In contrast, microporous scaffolds prepared by using NaCl as porogen appeared to have many homogeneously distributed pores of variable sizes, that frequently appeared to be interconnected (Fig. 1b). Sheets of microfibrous scaffolds prepared by the electrospinning technique were approximately 0.9 mm in thickness. They appeared as a complex meshwork of microfibres which were variable in diameter, 8–20 µm (Fig. 1c). Moreover, high magnification SEM micrographs clearly revealed rough surface and porosity of the microfibres (Fig. 1d).

Table 1 demonstrates peak stress (tensile strength) and peak strain for wall of the mouse stomach, compared to the three types of scaffold. Mouse stomach tissues had lower peak stress than all types of scaffold material. Closest peak stress to that of the stomach wall was the PCL microfibrous scaffold with 3-fold higher peak stress and 1.1-fold higher peak strain compared to that of stomach tissue. In contrast, non-porous and microporous scaffolds had much higher peak stresses (41.4 and 18.6, respectively, folds higher in value).

Table 1. Tensile performance of different polycaprolactone scaffolds and mouse stomach tissue

Samples	Peak stress (MPa)	Peak strain (%)
Non-porous scaffold	6.50 ± 1.20	13.7 ± 2.5
Microporous scaffold	2.93 ± 0.36	28.5 ± 5.0
Microfibrous scaffold	0.49 ± 0.12	162.5 ± 14.4
Mouse stomach tissue	0.15 ± 0.01	147.5 ± 9.5

Data presented as mean ± SD.

However, non-porous and microporous scaffolds exhibited much lower peak strain and lower flexibility under tensile testing compared to microfibrous scaffolds. Therefore, higher flexibility of microfibrous scaffolds makes them closer to natural gastric tissues than non-porous and microporous scaffolds. Proximity of microfibrous scaffolds in terms of mechanical properties, to native stomach tissue, makes them well suited for further study.

Viability and morphology of mGS cells cultured on different PCL scaffolds for 3 days (Experiment 1)

When mGS cells were seeded on non-porous, microporous and microfibrous PCL scaffolds and maintained for 3 days, cell population growth varied between the different scaffolds. Cell viability assays, using the live-cell stain calcein, showed that the microfibrous scaffold supported cell growth better than non-porous and microporous scaffolds (Fig. 2). Intensity of fluorescence produced by cells attached to the scaffold clearly demonstrated suitability of microfibrous scaffold for mGS cell growth. Statistical analysis of the data showed that cell viability was significantly higher ($P < 0.0001$) on microfibrous than non-porous or microporous scaffolds (Fig. 2).

Microscopic examination of toluidine blue-stained cells revealed their variable appearance on the different scaffolds used (Fig. 3a–c). On day 3, cells grown on non-porous and microporous scaffolds appeared at low density with only small colonies (Fig. 3a,b). However,

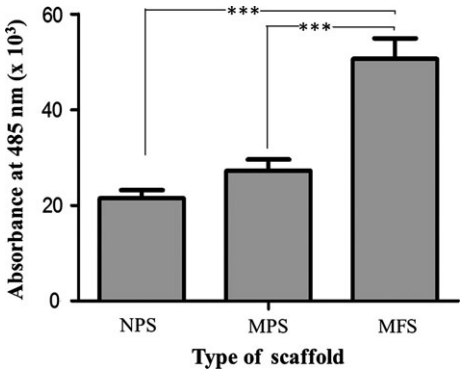

Figure 2. Cell viability assay for mouse gastric stem cells after 3 days of culture on non-porous (NPS), microporous (MPS) and microfibrous (MFS) polycaprolactone scaffolds. Note absorbance values (cell viability) are low in case of cells growing on NPS and MPS, but significantly increase in the case of MFS. Data expressed as mean ± SD. ***$P < 0.05$.

on microfibrous scaffolds, cells tended to appear at high density by day 3 (Fig. 3c).

Scanning electron microscope analysis was also used to characterize appearance of the cells and to describe their shape and size. On day 3, there were only few cells, small and stellate in shape with convex surfaces, on the non-porous and microporous scaffolds (Fig. 4a, b). When they were grown on microfibrous scaffolds, the cells were also small but appeared flattened (Fig. 4c).

Growth of mGS cells on microfibrous PCL scaffolds for 3–12 days (Experiment 2)

To evaluate population growth of mGS cells on microfibrous scaffolds, DNA was extracted and quantified at different time points using the PicoGreen assay. These data reflected number of cells attached and grown on the scaffolds. As shown in Fig. 5, measurements revealed that levels of DNA increased from 539 ng/ml (day 3) to 720 ng/ml (day 6), indicating proliferation of the attached mGS cells. However, when the cells were cultured for 9 days, amounts of DNA (reflecting the number of cells) was significantly lower ($P < 0.05$; Fig. 5). Reduction in the amount of DNA was also observed in cells cultured for 12 days with insignificant change in cell number (Fig. 5).

Morphological and immunocytochemical analysis of mGS cells cultured on microfibrous PCL scaffolds for 3 and 9 days (Experiment 3)

Scanning electron microscope examination of the mGS cells revealed that small size of mGS cells observed on

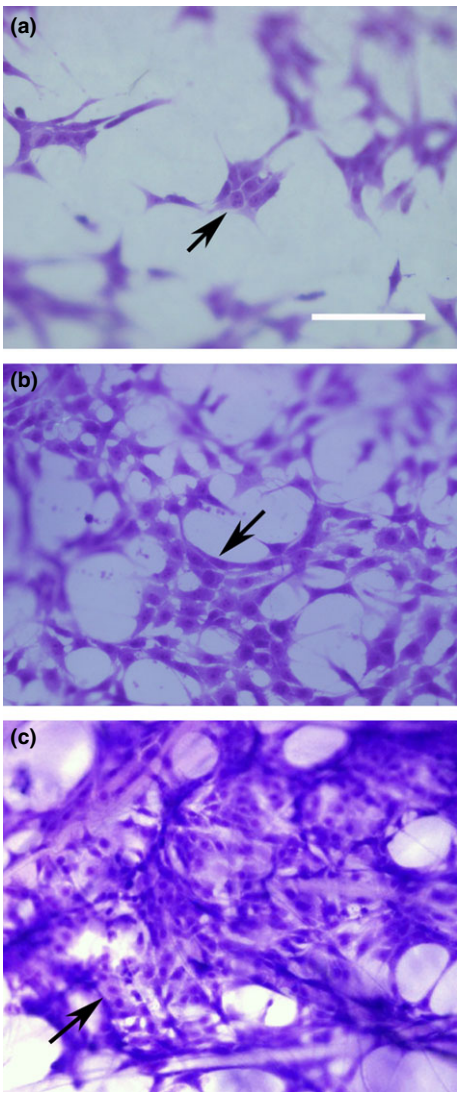

Figure 3. Light micrographs of toluidine blue-stained mouse gastric stem cells after 3 days culture on surfaces of non-porous (a), microporous (b) and microfibrous (c) polycaprolactone scaffolds. Arrows pointing to groups of mouse gastric stem cells stained with toluidine blue. Bar = 50 μm (a–c).

day 3 (Figs 4c,6a) was followed by their expansion and enlargement by day 9 (Fig. 6b). To test whether reduction in cell number and associated increase in cell size were due to cell differentiation, cryostat sectioning with lineage-specific lectin binding and immunocytochemistry were performed. Expressions of lineage-specific glycoconjugates and proteins were taken as measurement of cell differentiation. Microfibrous scaffolds with cells cultured for 3 and 9 days were sectioned at 10–30 μm and mounted on gelatin-coated slides. Some were stained with haematoxylin and eosin for light microscopy and general morphology (Fig. 7a). Adjacent sections were

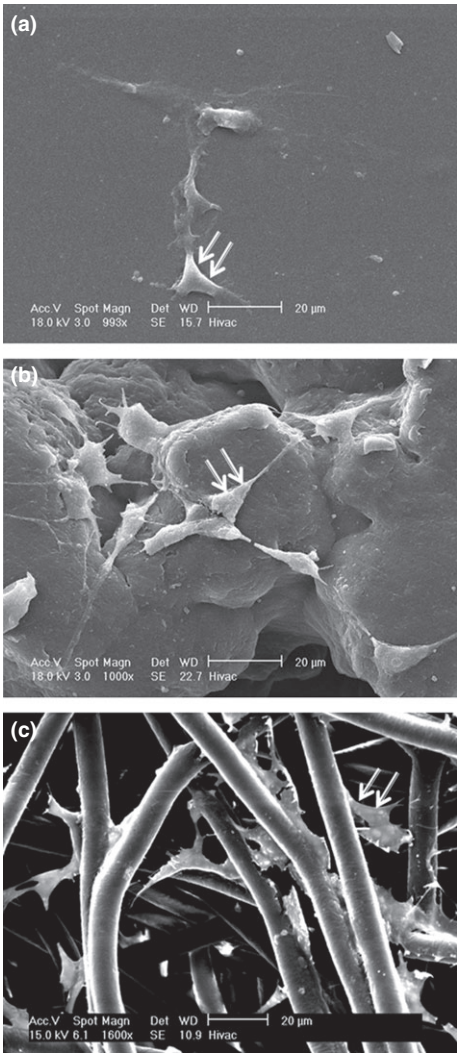

Figure 4. Scanning electron micrographs of mouse gastric stem cells cultured on non-porous (a), microporous (b) and microfibrous (c) polycaprolactone scaffolds for 3 days. Note stem cells (arrows) attached to each other and to surface of the scaffolds. Bar = 20 µm (a–c).

probed with fluorophore-conjugated lectins specific for different gastric epithelial cell lineages: surface mucous or pit cells (UEAI lectin), parietal cells (DBA lectin) and mucous neck cells (GSII lectin). Results showed that the cells bound neither to UEAI nor DBA lectins, but did bind to GSII lectin, as demonstrated with fluorescence microscopy (Fig. 7c) and confirmed with confocal microscopy (Fig. 7d). Immunoprobing using anti-TFF2 antibodies specific for mucous neck cells (29) revealed that after 9 days culture on microfibrous PCL scaffolds, some cells expressed TFF2 (Fig. 7b). Number of cells labelled with GSII lectin was counted in seven different images of cryosections obtained from the three

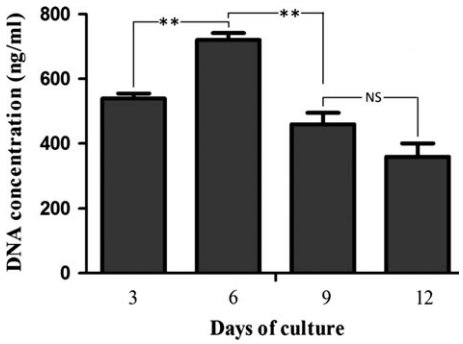

Figure 5. Estimation of DNA content of mouse gastric stem cells cultured on microfibrous polycaprolactone scaffolds for 3, 6, 9 and 12 days, using PicoGreen assay. Note DNA concentration (reflecting cell number) significantly increases from 3 to 6 days followed by a significant decline by days 9 and 12. Data expressed as mean ± SD. $^{**}P < 0.05$.

microfibrous scaffolds maintained in culture media for 9 days. Counts of total number of cells labelled with Hoechst and GSII lectin showed that approximately 50% of them had differentiated into mucous neck cells. Thus, it seems that PCL microfibrous scaffold is suitable for supporting not only growth of mGS cells but also their differentiation into mucus-secreting neck cells.

Discussion

This study describes an *in vitro* model system for population growth of mGS cells on synthetic biodegradable scaffolds, that support their differentiation into glandular mucous cells. This system is an advance toward establishing an engineered gastric mucosal tissue for use in regenerative treatment of gastric cancer/ulcer patients undergoing gastrectomy. As complete or even partial loss of the stomach may lead to devastating and life-threatening sequelae, the long-term plan of this research is to provide the basis for autologous or syngeneic transplantation of engineered gastric tissues.

Adult stem cells have already shown promise for tissue engineering application, but it is important to characterize culture conditions, properties of scaffold platforms and growth of the seeded cells to result in a new functional tissue (10,30).

Preferential growth of mGS cells on microfibrous PCL scaffolds

In this study, population growth of mGS cells on the surface of PCL scaffolds with different morphologies was first evaluated. PCL material was chosen here because it is a well-known biodegradable polymer that has long been used in tissue engineering (13–15). When

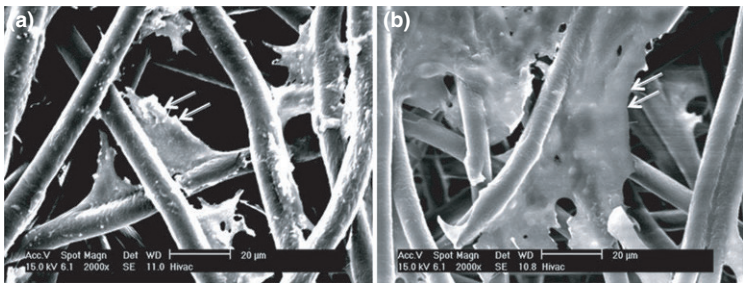

Figure 6. Microscopic analysis of mouse gastric stem cells growing on microfibrous polycaprolactone scaffolds. (a) Scanning electron micrograph of mouse gastric stem cells cultured for 3 days. Cells appear polyhedral or stellate (arrows) and adhere to the microfibres. (b) Scanning electron micrograph of mouse gastric stem cells (arrows) after 9 days culture. Cells expand and fill many of the spaces between microfibres. Bar = 20 μm (a, b).

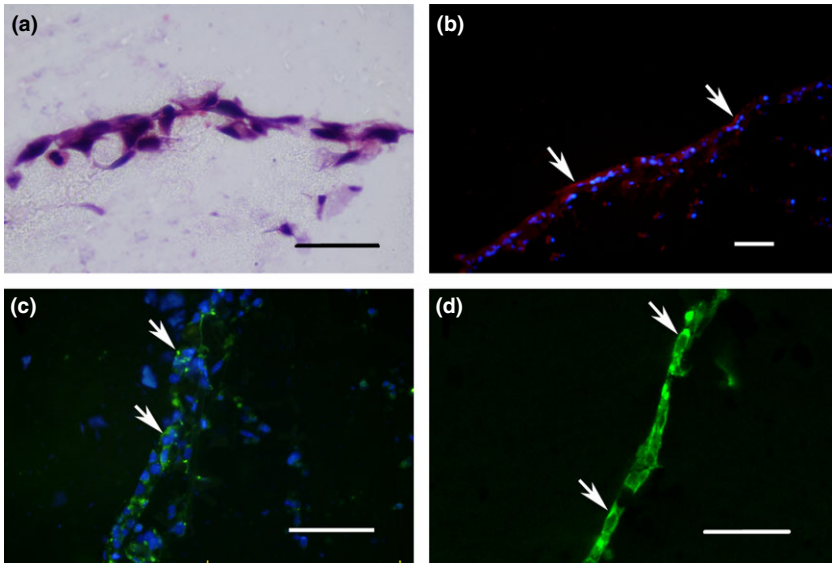

Figure 7. Microscopic analysis of mouse gastric stem cells growing on microfibrous polycaprolactone scaffolds for 9 days. (a) Light micrograph of cryostat section of mouse gastric stem cells stained with haematoxylin and eosin. (b) Fluorescence micrograph of cryostat section of mouse gastric stem cells probed with anti-TFF2 antibodies (red) and counterstained with Hoechst (blue). Arrows indicate TFF2-expressing cells. (c) Fluorescence micrograph showing GSII (green) binding and Hoechst (blue) nuclear labelling. Arrows indicate GSII-labelled cells. (d) Confocal micrograph confirming the cytoplasmic GSII (green) binding to cultured cells. Arrows indicate GSII-labelled cells. Bar = 50 μm (a–d).

mGS cells were equally seeded on different forms of PCL scaffold and incubated under the same conditions, cell viability assay (Fig. 2) and toluidine blue staining (Fig. 3) revealed that the microfibrous scaffold was better for cell population growth, than non-porous and microporous scaffolds. Having a scaffold made of PCL in a fibrous form provides all the virtues of high surface area on which cells can grow. In addition, having a non-woven fibrous scaffold of biodegradable PCL further provides interconnected porosity for cells to integrate and eventually form organized tissue.

The question arises whether the small number of cells growing on non-porous and microporous scaffolds would be associated with cell detachment and growth in suspension. To quantify both attached and possibly suspended viable mGS cells, MTT assay has been used (31). mGS cells were equally (1.6×10^6) seeded on 0.5 ml scaffolds (non-porous, microporous and microfibrous) and cultured for 3 days in 10% FBS-containing RPMI media in a 96-well plate. Formation of formazan, as a result of reducing tetrazolium salt by metabolically active mGS cells, was measured by spectrophotometry. Intensity of formazan provided a measure of total (floating and attached) viable mGS cells (Fig. 8). A pattern similar to that demonstrated with calcein assay was obtained; wells with microfibrous scaffolds had more viable cells than in non-porous or microporous scaffolds. These data support the results of the calcein assay and confirmed that microfibrous scaffolds enhance growth and proliferation of mGS cells. To further quantify cells attached to the surface of scaffolds and those in supernatant, the PicoGreen assay (described in the Materials and methods section) was used to estimate amounts of DNA of cells attached to the three different types of scaffold, after 3 days culture, compared to DNA of living or dead cells floating in the media. Amounts of

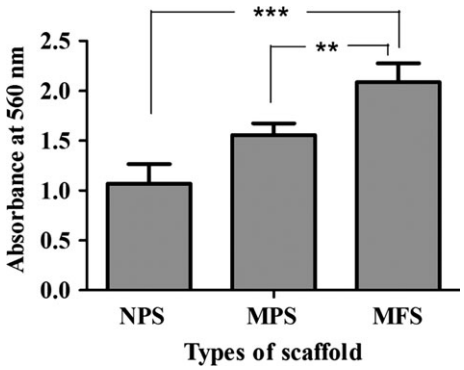

Figure 8. Estimation of total (attached and unattached) viable cells 3 days after their seeding on non-porous (NPS), microporous (MPS) and microfibrous (MFS) polycaprolactone scaffolds using MTT assay. Data plotted using Graph Pad Prism software and expressed as mean ± SD. ***$P < 0.0001$; **$P < 0.05$.

DNA from attached cells of microfibrous scaffolds was more than double of that of non-porous or microporous scaffolds. However, amounts of DNA of floating cells with non-porous scaffolds was more than triple those of DNA of microfibrous scaffolds. A summary conclusion of these assays after 3 days culture is diagrammatically presented in Fig. 9.

By using different cell viability assays and DNA quantification methods, it was possible to demonstrate and confirm preferential growth of mGS cells on microfibrous scaffolds. Non-porous PCL scaffold provided surface roughness which allowed adhesion and moderate proliferation of cells (32). Microporous scaffolds prepared with the salt-leaching method led to formation of pores that appeared to moderately facilitate growth and integration of cells on their surfaces (33). Microfibrous scaffolds fabricated by the electrospinning technique were the most suitable for growth of mGS cells for several reasons: (i) scaffolds acquired microsize pores with interconnectivity that aid communication between cells during their growth and proliferation, (ii) microfibres acquired surface roughness due to evaporation of solvent during their deposition, with high surface area under the effect of high voltage (32). This surface roughness enhances cell adhesion, (iii) the microfibrous scaffold offered a 3D construct with larger surface area than that of non-porous or microporous scaffolds, due to interlocking between the non-woven microfibres leading to various shapes and sizes of interconnected pores, (iv) the microfibrous scaffold had closer similarity in mechanical performance, when subjected to tensile forces, to that of natural stomach tissues and (v) this similarity could be attributed to the morphological appearance of microfibres of the scaffold which resemble fibres of extracellular matrix in connective tissue of the stomach wall (34). In this study, the average diameter of the fibres fabricated in the microfibrous scaffolds is within the normal range of collagen type 1 fibres of natural extracellular matrix.

Preferential growth of mGS cells on microfibrous scaffold is not surprising. Recently, Carlson *et al.* found that fibrous architecture of synthetic polymer scaffolds allows stem cells to develop a self-contained microenvironment that supports their proliferation, self-renewal and even differentiation, in combination with soluble

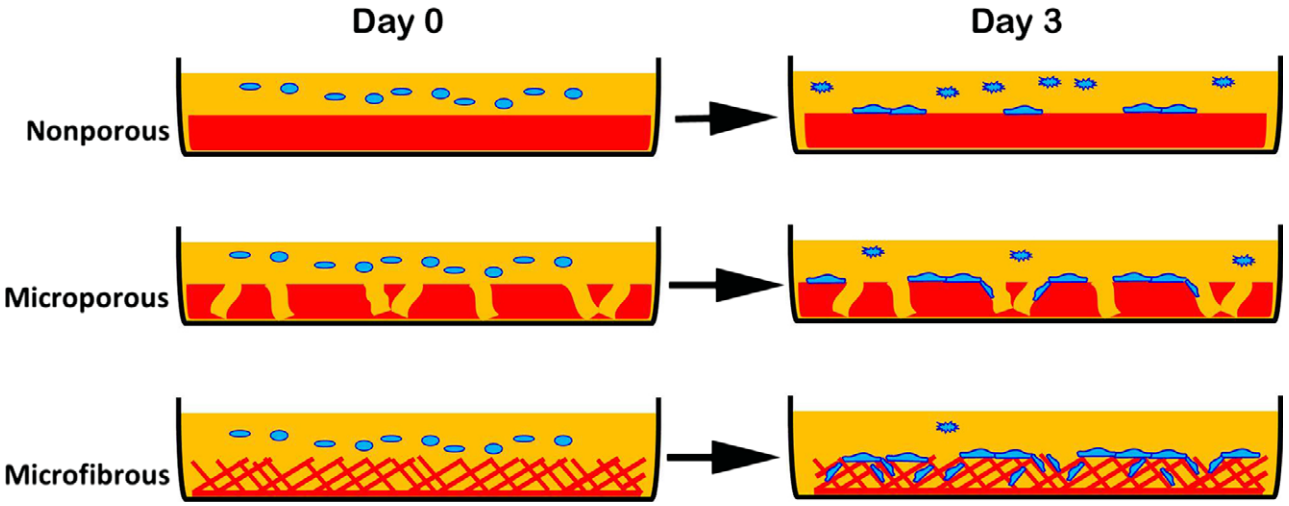

Figure 9. Schematic representation of mouse gastric stem (mGS) cell growth on non-porous, microporous and microfibrous polycaprolactone scaffolds for 3 days. Initially (day 0), equal number of mGS cells were seeded on the three scaffolds. By day 3, more cells were attached to the microfibrous scaffold than those on non-porous or microporous. However, numbers of floating (unattached) cells in culture media of non-porous scaffold are higher than those on microporous or microfibrous scaffolds. Thus, mGS cells appear to preferentially attach and grow on microfibrous polycaprolactone scaffold. This could be explained by increased surface area provided by random arrangement of microfibres that allows cell attachment and integration.

cues (35). They predicted that their findings would make it possible for stem cells to bypass the need for incorporation of matrix proteins or feeder cells.

Differentiation of mGS cells on microfibrous PCL scaffolds

Increased DNA content (proliferation) of mGS cells from 3 to 6 days culture on PCL scaffolds was followed by a significant reduction of DNA by day 9, suggesting a reduction in cell proliferation rate (Fig. 5). This was associated with increase in cell size of 9-day-cultured mGS cells compared to those of day 3 (Fig. 6). This change in cell size and cell number in day 9-cultured cells suggests a change in phenotype or differentiation of the mGS cells, with loss of some of these differentiated or end cells. To further clarify this observation, cryosections of cells cultured for 3 and 9 days were processed for lectin- and immunocytochemical probing. At 3 days culture, cells did not react with any of the gastric epithelial cell lineage-specific biomarkers examined. However, the situation was different for cells cultured for 9 days. Of the various lectins that are known to be markers for different gastric epithelial cells, GSII had reactivity with some of the cultured cells (Fig. 7). Lectin probing using UEAI and DBA were both negative (data not shown). It is well established that GSII binds to *N*-acetyl-D-glucosamine of mucous granules in glandular cells of the oxyntic/pyloric regions of the mouse stomach (29). Furthermore, when antibodies specific for TFF1, TFF2 and alpha/beta subunits of H,K-ATPase (respectively specific for pit, neck and parietal cells) were used for immunofluorescence probing, only anti-TFF2 antibodies reacted with some of the cells cultured for 9 days (Fig. 7). Immunoprobing analyses using anti-TFF1 and anti-H,K-ATPase antibodies were negative (data not shown). Also, cells grown on coverslips or chamber slides did not bind to any of the biomarkers examined. As both GSII lectin and anti-TFF2 antibody are known markers of glandular mucous cells, it appears that the mGS cells had differentiated into mucus-secreting cells.

These results could certainly be strengthened with quantitative RT-PCR using primers specific for TFF2 and Muc6 genes. However, it might be challenging to extract RNA from mGS cells cultured on hydrophobic PCL microfibrous scaffold (specially from those cells integrated deeply into the interconnected 3D spaces between microfibres). Such assay will require careful standardization and may even complicate the study, as it is well documented that positive RT-PCR will not always correlate with levels of protein (36) and we have already confirmed mGS cell differentiation into glandular mucous cells using different techniques. Results of both immunohistochemisty and lectin histochemistry demonstrated binding of two very well-characterized biomarkers, anti-TFF2 antibody (29) and GSII lectin (27,28). It is also known that gastric stem cell differentiation into a glandular mucous cells involves increase in cell size due to development of the machinery necessary for production of secretory granules (36). Indeed in this study, not only SEM revealed an increased cell size (Fig. 6) but confocal microscopy also showed development of GSII-positive secretory granules (Fig. 10) characteristic of mucous cells. All these findings together provided strong evidence for differentiation of the mGS cells into glandular mucous cells.

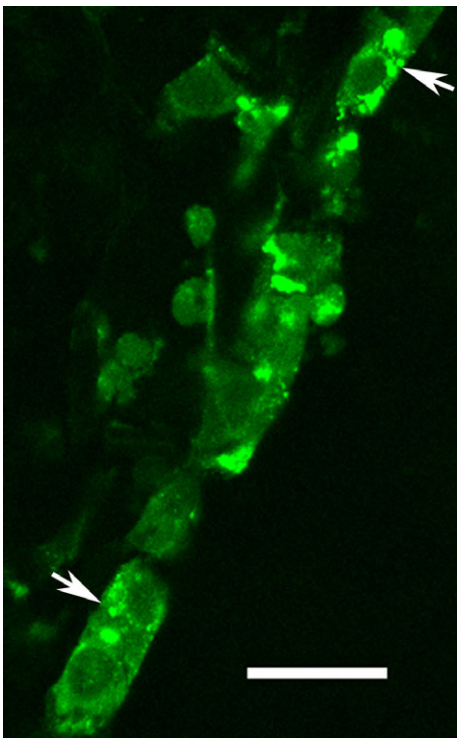

Figure 10. Confocal laser scanning micrograph demonstrating binding of GSII lectin (green) to cytoplasm of 9-day-cultured mouse gastric stem cells on microfibrous polycaprolactone scaffold. High magnification image demonstrates granular nature of labelled areas of cytoplasm, as expected from a mucus-secreting cell. Arrows indicate GSII-labelled cytoplasmic granules. Bar = 25 μm.

Little is known concerning molecular mechanisms involved in differentiation of mucus-secreting cells. In the corpus region of the mouse stomach, differentiation of stem cells into mucus-secreting neck cells is followed by their transformation into pepsinogen-secreting chief (zymogenic) cells (37). The transcription factor Mist1 has been identified as a regulator of differentiation of mucous neck cells into zymogenic cells (38). In addition, transcription factor XBP1 is required for turning off progenitor features of neck cells and induction of Mist1 (39).

There is indication supporting the view that transcription factor Blimp1 is an upstream regulator of, and is required for, XBP1 expression (40). In the mouse antrum and corpus, transcription factor Spdef is expressed in mucus-secreting gland/neck cells and is required for terminal differentiation of antral gland mucous cells (41). Whether Spdef or other molecules are involved in differentiation of mGS cells into mucus-secreting cells requires further analysis. This 3D culture system will, hopefully, help in defining molecular mechanisms involved in differentiation of gastric stem cells to mucus-secreting cells, as well as other gastric cell lineages.

Collectively, results of this study indicate that microfibrous PCL scaffolds support growth of mGS cells and trigger their differentiation into mucus-secreting glandular cells. This 3D culture system which utilizes microfibrous PCL scaffolds and normal culture media, without any additional growth factors, will help in establishing a model for gastric epithelial tissue engineering.

Acknowledgements

This study was supported by grants from UAE University and National Research Foundation. The technical assistance of Mr Saeed Tariq (Electron Microscopy Unit, UAEU) is highly appreciated. Antibodies specific for TFF1 and TFF2 were kindly provided by Dr Catherine Tomasetto (IGBMC, Strasbourg). The authors are grateful to Dr Keith Bagnall for the critical comments and discussions.

References

1 Karam SM, Leblond CP (1993) Dynamics of epithelial cells in the corpus of the mouse stomach. I. Identification of proliferative cell types and pinpointing of the stem cell. *Anat. Rec.* **236**, 259–279.
2 Karam SM, Straiton T, Hassan WM, Leblond CP (2003) Defining epithelial cell progenitors in the human oxyntic mucosa. *Stem Cells* **21**, 322–336.
3 Syder AJ, Karam SM, Mills JC, Ippolito JE, Ansari HR, Farook V *et al.* (2004) A transgenic mouse model of metastatic carcinoma involving transdifferentiation of a gastric epithelial lineage progenitor to a neuroendocrine phenotype. *Proc. Natl. Acad. Sci. USA* **101**, 4471–4476.
4 Farook VS, Alkhalaf M, Karam SM (2008) Establishment of a gastric epithelial progenitor cell line from a transgenic mouse expressing the simian virus 40 large T antigen gene in the parietal cell lineage. *Cell Prolif.* **41**, 310–320.
5 Giannakis M, Chen SL, Karam SM, Engstrand L, Gordon JI (2008) Helicobacter pylori evolution during progression from chronic atrophic gastritis to gastric cancer and its impact on gastric stem cells. *Proc. Natl. Acad. Sci. USA* **105**, 4358–4363.
6 Al-Marzoqee FY, Khoder G, Al-Awadhi H, John R, Beg A, Vincze A *et al.* (2012) Upregulation and inhibition of the nuclear translocation of Oct4 during multistep gastric carcinogenesis. *Int. J. Oncol.* **41**, 1733–1743.
7 Al-Awadhi H, John R, Al-Marzooqi F, Vincze A, Branicki F, Karam SM (2011) Sequential alterations in gastric biopsies and tumor tissues support the multistep process of carcinogenesis. *Histol. Histopathol.* **26**, 1153–1164.
8 Ferro A, Peleteiro B, Malvezzi M, Bosetti C, Bertuccio P, Levi F *et al.* (2014) Worldwide trends in gastric cancer mortality (1980–2011), with predictions to 2015, and incidence by subtype. *Eur. J. Cancer* **50**, 1330–1344.
9 Bolton JS, Conway WC 2nd (2011) Postgastrectomy syndromes. *Surg. Clin. North Am.* **91**, 1105–1122.
10 Jaklenec A, Stamp A, Deweerd E, Sherwin A, Langer R (2012) Progress in the tissue engineering and stem cell industry "are we there yet?". *Tissue Eng. Part B Rev.* **18**, 155–166.
11 Sethuraman S, Nair LS, El-Amin S, Farrar R, Nguyen MT, Singh A *et al.* (2006) In vivo biodegradability and biocompatibility evaluation of novel alanine ester-based polyphosphazenes in a rat model. *J. Biomed. Mater. Res. A* **77**, 679–687.
12 Nair LS, Lee DA, Bender JD, Barrett EW, Greish YE, Brown PW *et al.* (2006) Synthesis, characterization, and osteocompatibility evaluation of novel alanine-based polyphosphazenes. *J. Biomed. Mater. Res. A* **76**, 206–213.
13 Kweon H, Yoo MK, Park IK, Kim TH, Lee HC, Lee HS *et al.* (2003) A novel degradable polycaprolactone networks for tissue engineering. *Biomaterials* **24**, 801–808.
14 Williams JM, Adewunmi A, Schek RM, Flanagan CL, Krebsbach PH, Feinberg SE *et al.* (2005) Bone tissue engineering using polycaprolactone scaffolds fabricated via selective laser sintering. *Biomaterials* **26**, 4817–4827.
15 Woodruff MA, Hutmacher DW (2010) The return of a forgotten polymer polycaprolactone in the 21st century. *Prog. Polym. Sci.* **35**, 1217–1256.
16 Dai NT, Williamson MR, Khammo N, Adams EF, Coombes AG (2004) Composite cell support membranes based on collagen and polycaprolactone for tissue engineering of skin. *Biomaterials* **25**, 4263–4271.
17 Shor L, Güceri S, Wen X, Gandhi M, Sun W (2007) Fabrication of three-dimensional polycaprolactone/hydroxyapatite tissue scaffolds and osteoblast-scaffold interactions in vitro. *Biomaterials* **28**, 5291–5297.
18 Yeong WY, Sudarmadji N, Yu HY, Chua CK, Leong KF, Venkatraman SS *et al.* (2010) Porous polycaprolactone scaffold for cardiac tissue engineering fabricated by selective laser sintering. *Acta Biomater.* **6**, 2028–2034.
19 Grikscheit T, Srinivasan A, Vacanti JP (2003) Tissue-engineered stomach: a preliminary report of a versatile in vivo model with therapeutic potential. *J. Pediatr. Surg.* **38**, 1305–1309.
20 Maemura T, Shin M, Sato M, Mochizuki H, Vacanti JP (2003) A tissue-engineered stomach as a replacement of the native stomach. *Transplantation* **76**, 61–65.
21 Maemura T, Ogawa K, Shin M, Mochizuki H, Vacanti JP (2004) Assessment oftissue-engineered stomach derived from isolated epithelium organoid units. *Transplant. Proc.* **36**, 1595–1599.
22 Maemura T, Shin M, Kinoshita M (2013) Tissue engineering of the stomach. *J. Surg. Res.* **183**, 285–295.
23 Laurencin CT, Nair LS, Bhattacharyya S, Allcock HR, Bender JD, Brown PW *et al.* (2006) Polymeric Nanofibers for Tissue Enginering and Drug Delivery. US Patent No. 7235295.
24 Bhattacharyya S, Nair LS, Singh A, Krogman NR, Greish YE, Brown PW *et al.* (2006) Electrospinning of Poly[bis(ethyl alanato) phosphazene] Nanofibers. *J. Biomed. Nanotechnol.* **2**, 36–45.
25 Mourad AHI (2010) Thermo-mechanical characteristics of thermally aged polyethylene/polypropylene blends. *Mater. Des.* **31**, 918–929.

26 Mourad AHI, Mohamed F, Elleithy R (2009) Impact of some environmental conditions on the tensile, creep-recovery, relaxation, melting and crystallinity behaviour of UHMWPE GUR410- medical grade. *Mater. Des.* **30**, 4112–4119.
27 Falk P, Roth KA, Gordon JI (1994) Lectins are sensitive tools for defining the differentiation programs of mouse gut epithelial cell lineages. *Am. J. Physiol.* **266**, G987–G1003.
28 Karam SM, John R, Alpers DH, Ponery AS (2005) Retinoic acid stimulates the dynamics of mouse gastric epithelial progenitors. *Stem Cells* **23**, 433–441.
29 Karam SM, Tomasetto C, Rio MC (2004) Trefoil factor 1 is required for the commitment programme of mouse oxyntic epithelial progenitors. *Gut* **53**, 1408–1415.
30 Soleimani M, Nadri S, Shabani I (2010) Neurogenic differentiation of human conjunctiva mesenchymal stem cells on a nanofibrous scaffold. *Int. J. Dev. Biol.* **54**, 1295–1300.
31 Liu Y1, Peterson DA, Kimura H, Schubert D (1997) Mechanism of cellular 3-(4,5-dimethylthiazol-2-yl)-2,5-diphenyltetrazolium bromide (MTT) reduction. *J. Neurochem.* **69**, 581–593.
32 Biazar E, Heidari M, Asefnejad A (2011) The relationship between cellular adhesion and surface roughness in polystyrene modified by microwave plasma radiation. *Int. J. Nanomed.* **6**, 631–639.
33 Tessmar JKV, Holland TA, Mikos AG (2006) Salt leaching for polymer scaffolds: laboratory-scale manufacture of cell carriers. In: Ma PX, Elisseeff J, eds. Scaffolding in Tissue Engineering, pp. 111–124. Boca Raton, FL: Taylor & Francis.
34 Madurantakam PA, Cost CP, Simpson DG, Bowlin GL (2009) Science of nanofibrous scaffold fabrication: strategies for next generation tissue-engineering scaffolds. *Nanomedicine (London)* **4**, 193–206.
35 Carlson AL, Florek CA, Kim JJ, Neubauer T, Moore JC, Cohen RI *et al.* (2012) Microfibrous substrate geometry as a critical trigger for organization, self-renewal, and differentiation of human embryonic stem cells within synthetic 3-dimensional microenvironments. *FASEB J.* **26**, 3240–3251.
36 Vilmar A1, Garcia-Foncillas J, Huarriz M, Santoni-Rugiu E, Sorensen JB (2012) RT-PCR versus immunohistochemistr for correlation and quantification of ERCC1, BRCA1, TUBB3 and RRM1 in NSCLC. *Lung Cancer* **75**, 306–312.
37 Karam SM, Leblond CP (1993) Dynamics of epithelial cells in the corpus of the mouse stomach. III. Inward migration of neck cells followed by progressive transformation into zymogenic cells. *Anat. Rec.* **236**, 297–313.
38 Ramsey VG, Doherty JM, Chen CC, Stappenbeck TS, Konieczny SF, Mills JC (2007) The maturation of mucus-secreting gastric epithelial progenitors into digestive-enzyme secreting zymogenic cells requires Mist1. *Development* **134**, 211–222.
39 Huh WJ, Esen E, Geahlen JH, Bredemeyer AJ, Lee AH, Shi G *et al.* (2010) XBP1 controls maturation of gastric zymogenic cells by induction of MIST1 and expansion of the rough endoplasmic reticulum. *Gastroenterology* **139**, 2038–2049.
40 Shaffer AL, Shapiro-Shelef M, Iwakoshi NN, Lee AH, Qian SB, Zhao H *et al.* (2004) XBP1, downstream of Blimp-1, expands the secretory apparatus and other organelles, and increases protein synthesis in plasma cell differentiation. *Immunity* **21**, 81–93.
41 Horst D, Gu X, Bhasin M, Yang Q, Verzi M, Lin D *et al.* (2010) Requirement of the epithelium-specific Ets transcription factor Spdef for mucous gland cell function in the gastric antrum. *J. Biol. Chem.* **285**, 35047–35055.